Machine Vision-Based Assessment of Fall Color Changes and its Relationship with Leaf Nitrogen Concentration

Achyut Paudel^a, Jostan Brown^b, Priyanka Upadhyaya^a, Atif Bilal Asad^a, Safal Kshetri^a, Joseph R. Davidson^b, Cindy Grimm^b, Ashley Thompson^c, Bernardita Sallato^a, Matthew D. Whiting^a, Manoj Karkee^a

Abstract

Apple trees, being deciduous, shed leaves each year. This process is preceded by the change in leaf color from green to yellow (also known as senescence) during the fall season. The rate and timing of color change are affected by factors including nitrogen (N) concentration in leaves. The green color of leaves and the speed at which it turns yellow during senescence are highly dependent on chlorophyll content, which in turn depends on nitrogen concentration in the leaves. The assessment of leaf color during this period can therefore provide important information on the nitrogen status of apple trees. This study focused on a machine vision-based system to quantify the timing and change in leaf color during the fall and correlate that information to leaf nitrogen content. The color and 3D image dataset used in this study was collected over five weeks in the fall of 2021 and 2023 at a commercial orchard (tall spindle architecture) using a ground-vehicle-based stereo vision sensor. First, the point cloud obtained from the sensor was used to segment the tree canopies using color and depth thresholding methods in the natural orchard environment. Then, the color information of the segmented canopy area was quantified using a custom-defined metric, yellowness index (a normalized ratio of yellow to green foliage in the tree) that varied from -1 to +1(-1 being completely green and +1 being completely yellow), which gives the proportion of yellow leaves on a tree. A K-means-based method and a gradient boosting method were used to estimate the yellowness index. The gradient boosting method proposed in this study was

^a Biological Systems Engineering Department, Center for Precision and Automated Agricultural System, Washington State
University, Prosser, 99350, WA, USA

^b Collaborative Robotics and Intelligent Systems Institute, , Oregon State University, Corvallis, 97331, OR, USA ^c Mid-Columbia Agricultural Research and Extension Center, , Oregon State University, Hood River, 97031, OR, USA

found to be superior to the K-means-based method, achieving an R^2 of 0.72 in estimating the *yellowness index*. The results showed that the metric was able to capture the gradual color transition from green to yellow over the study period. It was also observed that the trees with lower nitrogen showed the color transition to yellow earlier than the trees with higher nitrogen. The onset of color transition during both years aligned with the 29th week post-full bloom. This critical timing could be used for conducting nitrogen status analysis on apple trees using machine vision, enabling more precise and timely assessment of nutrient levels and facilitating targeted fertilization strategies in orchard management.

Keywords: Leaf Nitrogen, Machine Vision in Agriculture, Point Cloud Segmentation, Precision Nitrogen Management, Machine Learning in Agriculture

1. Introduction

Currently, tree fruit orchards are managed at at block or field level providing inputs such as water and nutrients uniformly to hundreds or even thousands of trees in the block without addressing the needs of individual trees. This coarse management of crops often leads to sub-optimal inputs thus negatively impacting tree growth, yield, and fruit quality (Klein et al., 1989; Neilsen et al., 2009). Individual tree-level management in tree fruit crops such as apple orchards presents a promising frontier for significantly enhancing fruit yield and quality addressing the unique needs of individual trees. However, managing these orchards (Figure 1) at the individual tree level is challenging, particularly in terms of assessing the needs of individual trees and making precise management decisions. Each tree within an orchard is unique with its specific needs for water, nutrients, and other inputs (Aggelopoulou et al., 2010; James A. Taylor et al., 2007). This variability can be caused by multiple factors including spatial variation of soil properties like texture, depth, slope, and microbial activities, and variation in microclimate within orchards (Aggelopoulou et al., 2010; Umali et al., 2012; Cho, 2010). Effective input management at the individual tree level could be possible if crucial factors such as nitrogen and water availability to individual trees can be

accurately assessed.



Figure 1: A representative high density apple orchard plantation in Prosser, Washington. The trees have been trained in a tall spindle architecture and spaced closely (4 foot) forming a highly dense planar "wall".

Nitrogen (N) is a major input to apple trees that impacts growth, health, and fruit quality (Sanchez et al., 1995). Traditionally, the most accurate approach to assess tree N status involves laboratory-based leaf and soil nitrogen measurement, which provides a quantitative baseline for assessing the need for nitrogen application. However, these methods demand significant time and expense (Baret and Fourty, 1997), limiting sampling density and the possibility of individual tree-level management in commercial orchards. As a result, orchard management often relies on data collected from sparingly located sample trees or sampling locations, lacking precision due to inherent spatial variations within orchards (Ferguson and Triggs, 1990; Wulfsohn et al., 2012; Arnó et al., 2017)

These limitations of both laboratory-based and visual assessment methods underscore the need for a rapid, reliable, and more comprehensive approach to N status evaluation (Cheng and Schupp, 2004) at individual tree level. A machine vision-based system offers a

promising solution by automating and standardizing the quantification of visual parameters across entire orchards. This approach could provide objective, quantifiable data that can be correlated with nitrogen status through various models. By enabling more precise, tree-level management in commercial orchards, such a system has the potential to overcome the sampling and subjectivity issues inherent in current methods while offering scalability for broader applications.

Machine vision techniques have been extensively used to acquire various canopy-level features and stresses in fruit crops (Wang et al., 2023; Paudel et al., 2022; Wachs et al., 2010; Wang et al., 2018; Brown et al., 2024). Specifically, many recent studies have reported machine vision-based tools for estimating canopy density(Mahmud et al., 2021; Paudel et al., 2023), tree trunk cross-sectional area (Wang et al., 2023), and canopy color (Naschitz et al., 2014) in fruit trees.

Leaf color is one of the key canopy characteristics that is correlated to nitrogen content (Ali et al., 2012; Treder et al., 2016; Ye et al., 2020). This correlation is primarily due to the presence of chlorophyll in leaves. Chlorophyll, the pigment responsible for photosynthesis, contains nitrogen as a key component of its molecular structure. It reflects light primarily in the green spectrum, which is why leaves appear green to our eyes. In deciduous trees like apples, a significant color change occurs as the growing season progresses towards fall. This change is primarily due to the relocation of nitrogen from leaves to woody regions for storage and to support spring growth (Murneek and Logan, 1932; Spencer, 1973). As chlorophyll breaks down and moves back into the tree, the leaves transition from green to yellow.

This color transition provides a visual indicator of the tree's nitrogen status. A greener canopy with vigorous growth is often correlated with a tree having high nitrogen, while a yellower and less vigorous canopy is often associated with trees with low nitrogen (Raese et al., 2007; Lee, 2002). Trees with very high nitrogen tend to maintain their green color longer into the season. The canopy color during this critical transition period can provide a

unique and accurate indicator of tree nitrogen status.

While various RGB, multispectral, and hyperspectral imaging techniques have been used in the past to quantify the color to estimate nitrogen or chlorophyll content in leaves, most studies have focused on crops in controlled environments and at the individual leaf level. This focus limits their applicability to outdoor orchard conditions. Our study addresses this gap by using the images in natural orchard environments, and at the whole canopy level. We also aim to quantify canopy color over a senescence period when color difference in the tree foliage is more apparent, which can be used to assess nitrogen status of each tree in commercial orchards, potentially enabling precision management practices at the individual tree level.

Specifically, this study tracked apple tree canopies over five weeks in fall using RGB-D cameras, quantifying their color within an outdoor orchard environment and related the color at those critical periods of transition to the nitrogen levels in the corresponding trees. Specifically, the study focused on the following two research objectives:

- 1. To develop a machine vision-based technique to quantify foliage color during late fall in an outdoor apple orchard.
- 2. To use the foliage color to differentiate between trees with varying foliage nitrogen concentration.

The rest of the paper is structured into three sections. Section 2 details the data collection and processing methodologies. Section 3 delves into the results, offering insightful interpretation and pertinent discussion surrounding their emergence. Finally, Section 4 summarizes the key findings with discussions about the current limitations and future potentials.

2. Materials and Methods

The overall data collection and processing method used in this study is shown in Figure

2. Further detail about each step has been explained in the subsequent sections. The study

consisted of collecting RGB-D images over multiple weeks in fall 2021 and 2023. The point cloud data of the tree canopies were then segmented into yellow and green foliage and a metric - yellowness index was defined and estimated to quantify the color of the trees. The yellowness indices of the tree during different weeks was then correlated to the leaf nitrogen content for each year.

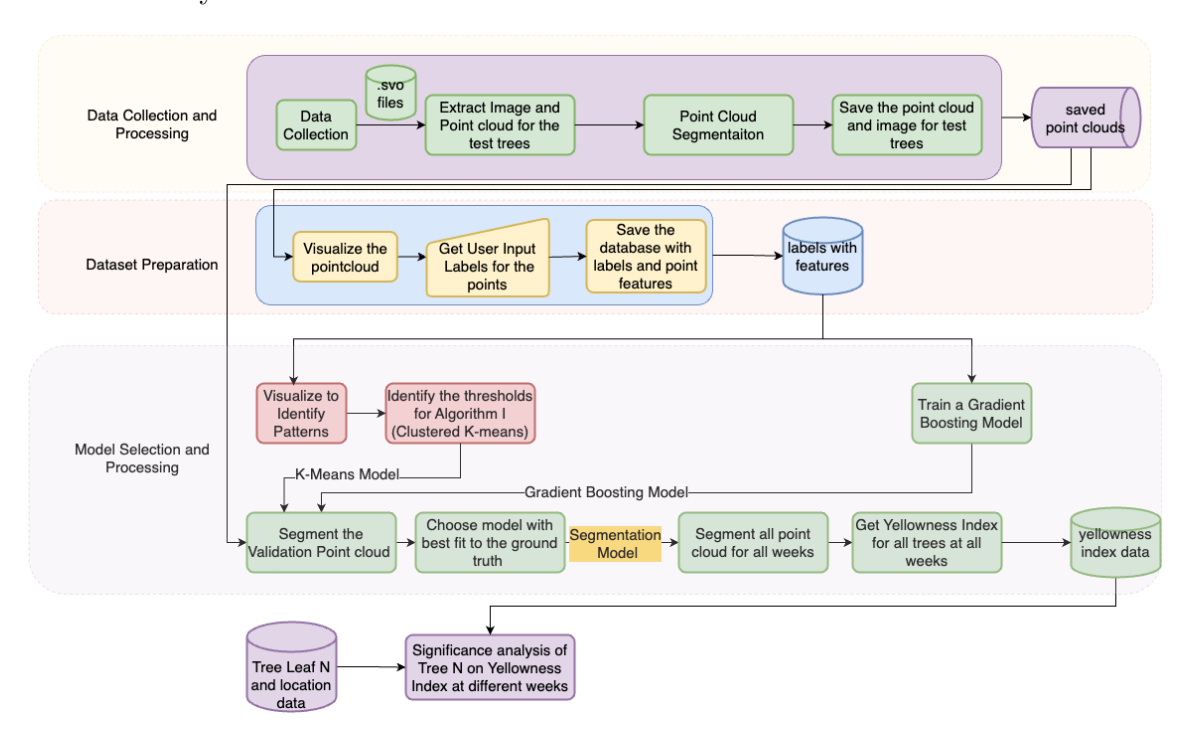


Figure 2: Overall Data collection and processing method for the study. Each light colored box represent a distinct process and has been described further in subsequent sections.

2.1. Data Collection

The dataset (color and 3D images) for this study was collected over five weeks in Fall, 2021 (from October 13 to November 14) and Fall, 2023 (from October 20 to November 17). These images were collected in a Jazz[™] commercial orchard (Yakima Valley Orchard) in Prosser, WA (Figure 3). Start day of the data collection was determined by when the leaves started to change the colors from green to yellow (Figure 4), also known as senescence. A total of 200 sample trees were scattered across 17 rows of the test orchard, with every 3rd tree in each row of trees taken as a sample. The data was collected using a commercial stereo-vision-

based RGB-D camera (Zed2i, Stereolabs, Paris, France) mounted on a utility vehicle (Figure 3b). The trees were trained to a vertical structure using a tall spindle canopy architecture (Figure 1). The camera was mounted 7 feet above the ground to ensure the majority of the canopy was visible. An SVO file (Stereolabs file format) with all the metadata including the camera parameters, images, and sensor data was recorded for each row of trees. Images (pixel resolution of 2208 x 1242) and point cloud (maximum depth of 10m) for each tree were later extracted based on timestamp matching between frames and user input. During processing, the RGB and co-registered point cloud were identified for each test tree.

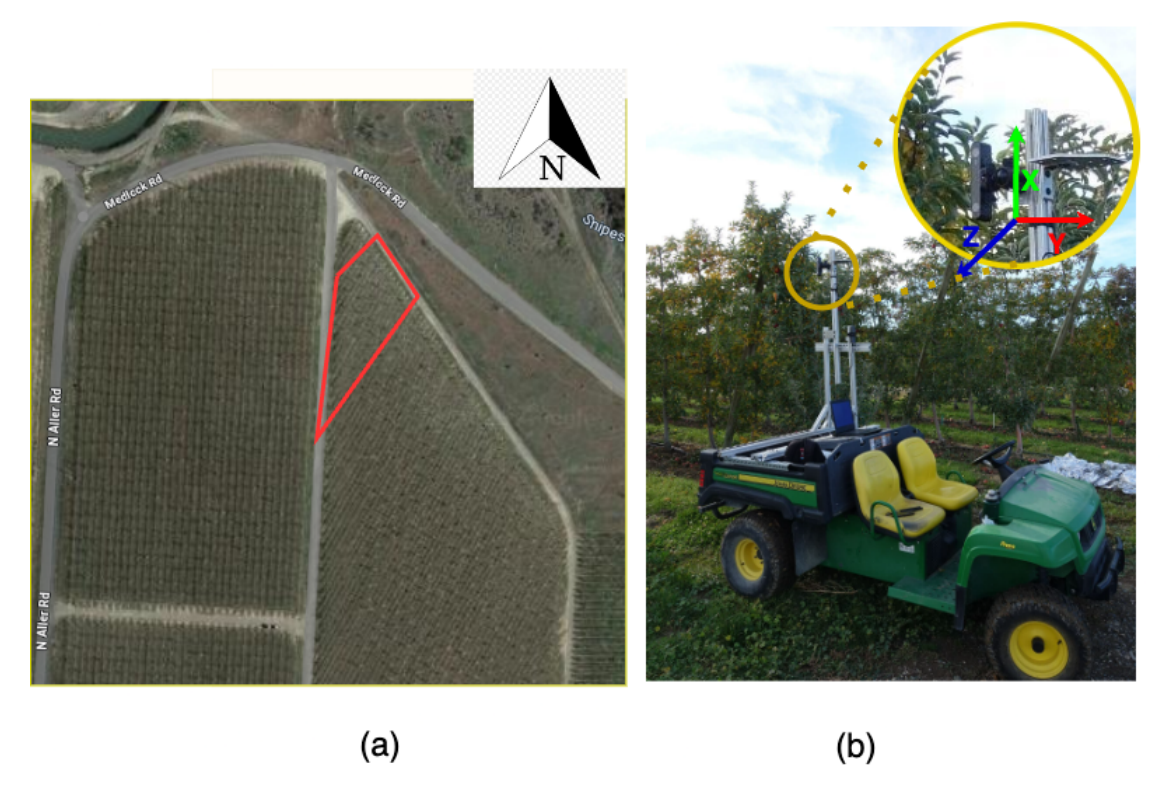


Figure 3: Study site and sensing setup; (a) A satellite view of the test plot. The red outline shows the location of the plot used in this study., and b) Ground vehicle with a camera mounted on top (zoomed portion shows camera and axes orientations),

2.2. Point Cloud Processing and Segmentation

2.2.1. Foreground Tree Segmentation

The initial data acquired through the stereovision sensor was noisy and required further refinement. An initial step involved applying a color threshold of 153 to the blue channel to



Figure 4: Images of the same tree during different weeks of the data collection. The dates below represent the exact dates when the data was collected in 2023. The foliage can be seen gradually changing from green to yellow.

filter out pixels corresponding to the sky. Subsequently, a distance threshold of 3 meters along the Z-axis (depth axis), was implemented. The optimal threshold values were determined experimentally through trials and visual inspections. Consequently, the resulting point cloud consisted of points mostly from the foreground tree, with some residual points from the ground. To eliminate the undesirable ground points, the points within 50 centimeters above the lowest x-value (along the height of the tree) were excluded. The resulting point cloud was down-sampled by selecting every tenth point, effectively reducing its size while preserving essential information for subsequent analysis.



Figure 5: Schematic for point cloud segmentation and downsampling process used in the study

2.2.2. Color Segmentation and clustering

The point cloud obtained from step 2.2.1 consisted of points from the foreground tree, and could be broadly categorized into yellow leaves, green leaves, and the trunk. Data collection spanned multiple weeks, capturing the tree's seasonal shift during the fall color change,

depicted in Figure 4. consisted of points from the foreground tree, and could be broadly categorized into yellow leaves, green leaves, and the trunk. Data collection spanned multiple weeks, capturing the tree's seasonal shift during the fall color change, depicted in Figure (Figure 6a) and CIE-Lab* (Figure 6b and c) color spaces were used to reduce the effect of varying intensity. In the HSV space, hue remains unaffected by varying light intensity, while in the CIE-Lab* space, the a* and b* values correspond respectively to red-green and blue-yellow colors. RGB images captured by the RGB-D sensor were converted to both the CIE-La*b* (Lab) space, using a standard D65 illuminant, and the HSV color space. These conversions were performed using the scikit-image library (Van der Walt et al., 2014).

The transition of the trees from green to yellow color was noticeable in both HSV and La*b* space (Figures 6a and 6b,c). A probability density plot for the hue space across the weeks illustrated a decline from approximately 110 degrees in week 1 to about 50 degrees in week 6, signifying the shift from green to yellow. A similar trend was visible in the probability density plots for a* and b* in the La*b* space. Both a* and b* showed a slight increase as the weeks progressed, corresponding to a color change from green to yellow.

The transition in tree canopy color was apparent qualitatively, but a robust quantitative approach was needed to precisely quantify them. To achieve this, individual points in the point cloud were categorized into distinct groups of yellow leaves, green leaves, or the trunk. Qualitative analyses using K-means clustering over multiple samples in both the La*b* and HSV color spaces showed that the La*b* space performed better in distinguishing yellow and green pixels as separate classes. Consequently, the subsequent analysis was conducted using La*b* color space. To cluster the point cloud, a modified k-means algorithm (Algorithm 1) was applied, initially grouping the points into 20 clusters. A threshold for the cluster center was set in both the a* and b* space, to merge these clusters into three distinct classes: Yellow, Green, and Trunk. The Yellow cluster encompassed foliage that had transitioned to yellow, while the Green cluster comprised foliage that retained its green color. The Trunk

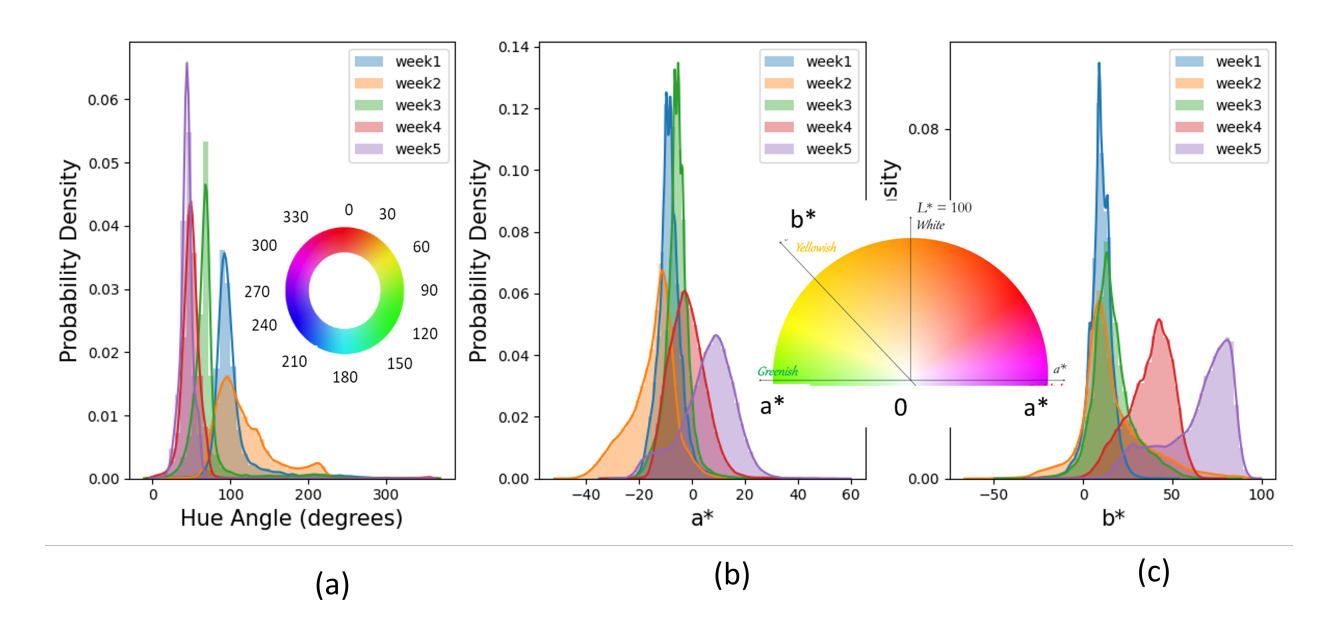


Figure 6: Distribution of a) Hue angles and b) a* and c) b* values for one of the sample trees during the five-week study period of 2023. The color chart shows the color associated with different values for (a) hue angles, (b) (Thompson, 2017) a*, and b*. The hue angle decreased in a) and a* and b* increased in b) and c) as the weeks progressed during the study all signifying the shift from green to yellow.

cluster included points from the trunk, branches, background soil, and some brown leaves.

A detailed breakdown of the clustering process is outlined in Algorithm 1.

Algorithm 1: Clustering of Point Cloud

Input: Point cloud from stereovision system, P

Output: Clustered Point cloud-3 groups, Green, Yellow, Trunk

- n = initial number of cluster (integer)
- **2** K-Means Clustering using a, b values into n clusters (c)
- **3** Green cluster $(c_g) = 0$; Yellow cluster $(c_y) = 0$; Trunk cluster $(c_t) = 0$
- 4 for i in range(n) do
- if $cg_{amin} < c_i(a) < cg_{amax}$ and $cg_{bmin}c_i(b) < cg_{bmax}$ then
- $c_q = c_q + c_i;$
- 7 else if $cy_{amin} < c_i(a) < cy_{amax}$ and $cy_{bmin}c_i(b) < cy_{bmax}$ then
- $c_y = c_y + c_i$
- 9 else if $ct_{amin} < c_i(a) < ct_{amax}$ and $ct_{bmin}c_i(b) < ct_{bmax}$ then
- $c_t = c_t + c_i$
- 11 end
- 12 end

13 return c_g , c_y , c_t

In the aforementioned algorithm, the manual setting of threshold values for a* and b* required multiple iterations to identify optimal values suitable across the data throughout the weeks. To standardize this process, a methodology involving manual user input labels was implemented to obtain a labeled dataset. A custom Python program (Figure 7), using the Open3D library (Zhou et al., 2018), was developed to label the point cloud. This interactive program allowed users to choose between three labels - 'Green', 'Yellow', and 'Trunk' and manually select the points belonging to these labels. Trees were randomly sampled throughout the entire data collection period, and the labels along with the characteristics of the points were recorded to create the dataset.

To visualize the difference between groups, a distribution plot of the a*, and b* spaces was

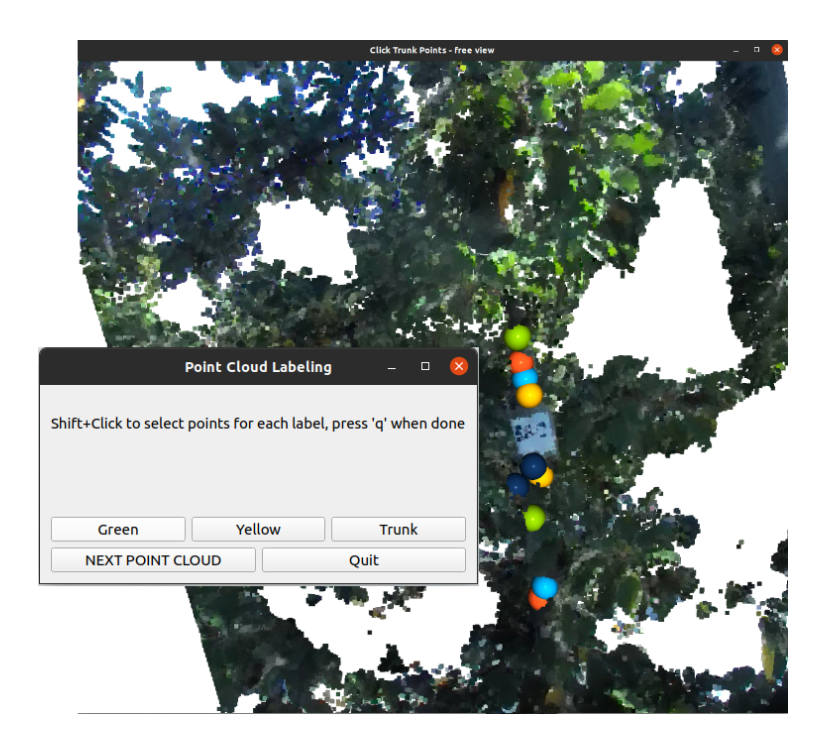


Figure 7: A custom program to select the points belonging to multiple classes - Green, Yellow, and Trunk. This instance showed an interactive window where the user selected points belonging to the trunk. The features of the points - including a*,b*,R, G, B, and their eigenvector and eigenvalues were recorded into a spreadsheet for further analysis.

created (Figure 8). These plots provided strategic reference points for selecting threshold values. For the 2023 dataset, the threshold values for a^* and b^* were determined as follows: $a^* < -10$, $0 < b^* < 25$ for Green, $b^* > 45$ for Yellow, and $a^* > 0$, $0 < b^* < 50$ for Trunk. While K-means clustering, being an unsupervised method, doesn't necessitate user inputs for training data and attempts to identify inherent clusters in the dataset, it comes with certain drawbacks. The method's main limitations include longer computation times due to the need to process all points and its reliance on random initialization, potentially leading to different solutions with each run.

An alternative approach utilized a gradient boost classifier, an ensemble learning technique that combines multiple weak learners (typically decision trees) to create a stronger, more robust model (Bartlett et al., 1998). It sequentially builds new models, focusing on correcting the errors made by the previous ones, ultimately producing a more accurate and powerful predictive model (Natekin and Knoll, 2013). In this study, the gradient boost classical errors are considered as a stronger, and a stronger are considered as a stronger.

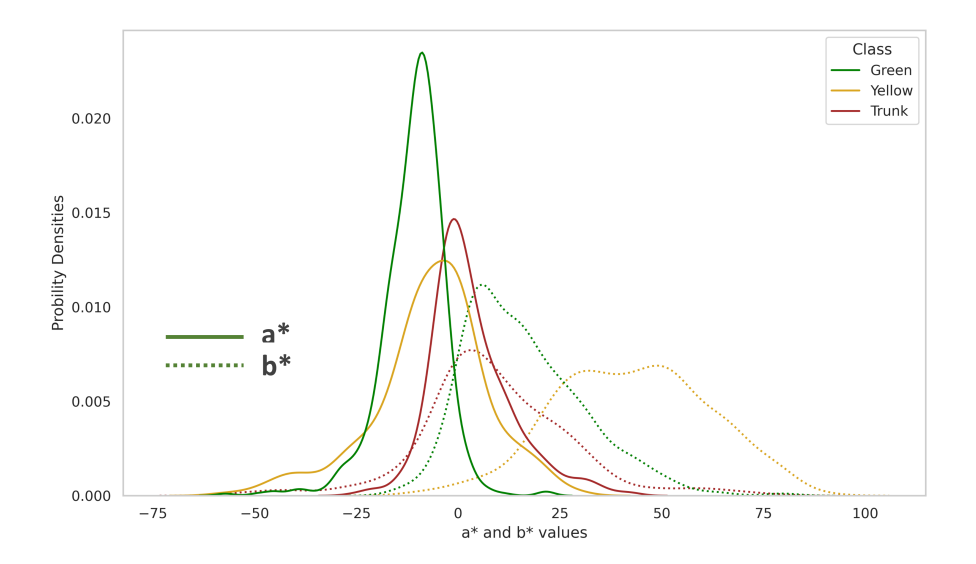


Figure 8: a* and b* values in CIE-L*a*b* space during different weeks of image acquisition (2023) for points belonging to green, yellow, and trunk classes. The solid lines represent a* values, and dotted lines represent b* values, different colors represent different classes.

sifier model was created using scikit-learn (Van der Walt et al., 2014). The dataset was divided into 80% training and 20% testing sub-sets. The model required tuning of different hyperparameters. A strategic approach to varying model hyperparameters was employed, with one hyperparameter held constant while varying the others to analyze their individual effects on model accuracy. The hyperparameter learning rate was varied between 0.1-1, max depth was varied between 1-5, and n estimator was varied between 100-1000 and their performance on training and test dataset was analyzed. The set of hyperparameters that achieved the highest accuracy on the test data was then selected.

The outputs from both Algorithm 1 (K-Means) and the Gradient Boosting method provided labels—'Green', 'Yellow', or 'Trunk'—for each point in the point cloud. Following the clustering of points, a metric, yellowness index, was used to quantify the extent of yellowing within each tree canopy. The yellowness index, calculated using Equation 1, represents the normalized ratio between yellow and green points within a tree canopy, with values ranging between -1 and +1. A value of -1 indicates that the tree was entirely green, while a value of +1 signifies complete yellowing.

$$yellowness\ index = \frac{y-g}{y+g} \tag{1}$$

where,

y = number of points with 'Yellow' label (c_y)

 $g = \text{number of points in 'Green' label } (c_g)$

To assess the performance of the yellowness estimation techniques, 50 validation trees were randomly selected and deleafed between the second and fourth trellis wires (a section of the trees, Figure 9). The leaves removed from each tree were collected in a bag and then later segregated manually into separate groups ("Green" or "Yellow") for each tree. A leaf was identified as 'Green' if more than half of the leaf area was green, and 'Yellow' if otherwise. The precise weights of the yellow and green leaf groups were measured using a highly accurate Mettler PC 4000 (Mettler Toledo, Switzerland) weighing scale. This value served as the ground truth to assess the models' performance. The yellowness index value was computed for all validation trees using Equation 1. Both Algorithm 1 and Gradient Boosting were evaluated against the ground truth data, with the superior-performing model based on this evaluation selected for further study.

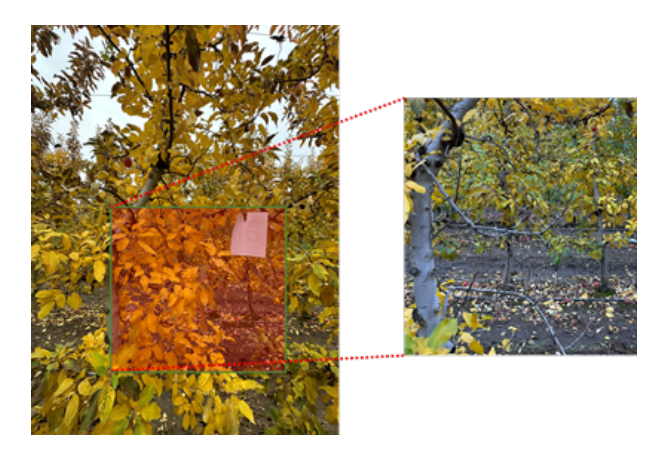


Figure 9: The image of the tree before and after deleafing. The leaves from the tree between the second and fourth trellis wire from the bottom (shown in transparent red box) were deleafed and collected.

2.3. Relationship between Yellowness Index and Leaf Nitrogen Concentration

To investigate if the yellowness index had any relationship with the foliar nitrogen concentration on the trees, the *yellowness index* values were regressed against the leaf nitrogen concentration. The leaf nitrogen concentration was obtained using the standard Kjeldahl's method (Kirk, 1950) by collecting 50 fully grown mid-shoot leaves from each tree, at the end of the growing season (Late July in 2021 and early August in 2023). The leaf nitrogen concentration would show the average nitrogen status of each tree and has been linked with various factors like canopy growth and canopy color. There are different recommendations on a good nitrogen level for trees depending on the variety (Cheng and Schupp, 2004; Cheng, 2010; Sallato, 2017; UniversityofArizona). The leaf nitrogen level of 2-2.4% was regarded as a good nitrogen level in this study for Jazz™ apple trees based on these recommendations.

A one-way ANOVA analysis was conducted to examine the yellowness values across various weeks, classifying trees into either 3 or 5 groups according to their leaf nitrogen concentrations. In the 3-class classification, trees were categorized as 'Low'(N < 2%), 'Good'(2% < N < 2.4%), and 'High'(N > 2.4%). Meanwhile, the 5-class classification included 'VeryLow'(N < 1.7%), 'Low'(1.7% < N < 2%), 'Good'(2% < N < 2.4%), 'High'(2.4% < N < 2.6%), and 'VeryHigh'(N > 2.6%) categories. The ANOVA analysis was followed up by a Tukey HSD posthoc analysis to analyze the significant difference between pairs of groups if ANOVA showed a significant difference.

A one-way ANOVA was performed to examine differences in the yellowness index among trees. This analysis was conducted separately for each week of the season, comparing trees grouped by their leaf nitrogen levels to determine if trees with different nitrogen statuses exhibited significant variations in their yellowness index throughout senescence. The trees were classified into 5 groups according to their leaf nitrogen concentrations: 'VeryLow'(N < 1.7%), 'Low'(1.7% < N < 2%), 'Good'(2% < N < 2.4%), 'High'(2.4% < N < 2.6%), and 'VeryHigh'(N > 2.6%). The ANOVA analysis was followed up by a Tukey HSD posthoc

analysis to analyze the significant difference between pairs of groups if ANOVA showed a significant difference.

3. Results and Discussions

3.1. Tree Segmentation and Clustering

The original colored point cloud was clustered into green and yellow groups to quantify the yellowness of each tree canopy in the test orchard. As discussed in the methods section, Algorithm 1 (K-means based) and Gradient Boost classifier were used to classify leaves into these two groups. For the Gradient Boost model, learning rate, max depth, and n estimator were varied to identify the best set of hyperparameters (Figure 11). It can be seen from the figure that the model started to overfit the training data on increasing the hyperparameters, as indicated by higher performance on the training set with reduced performance on the test set (eg, training accuracy went from 0.85 to nearly 1, while testing accuracy decreased as max_depth of the trees was varied from 1 to 3, Fig 11b). The gradient boost method with the best set of hyperparameters achieved an accuracy of 78% on the test set with a learning rate of 0.1, maximum depth of 1, and a number of estimators as 100.

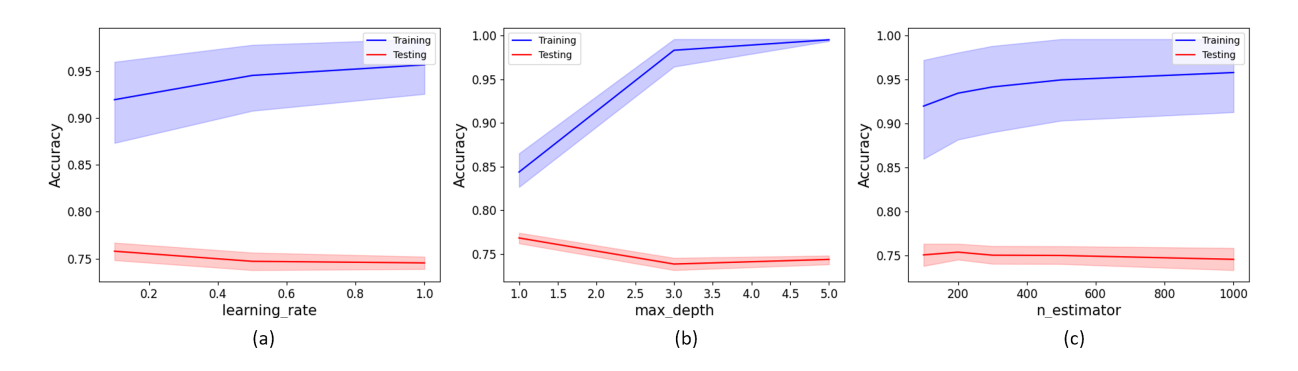


Figure 10: Varying accuracies for the gradient boost model with different combination of hyperparameters (a) Learning Rate, b) Maximum Depth of Tree, and c) Number of Estimators. The blue line denotes varying accuracy during training whereas the red line represents varying accuracy during testing. The shaded regions around the lines illustrate the range of accuracies across different values of the other hyperparameters, with the indicated hyperparameter being held constant.

The Gradient Boost model with the optimal hyperparameter configuration was compared

against Algorithm 1 to determine the superior method among two. The models were evaluated using the validation data, detailed in Section 2.2.2. Figure 11 qualitatively shows the performance of the two models within cropped canopy regions (between the second and fourth trellis wire). Quantitative assessment of the performance of these models was performed using the Yellowness Indices (calculated with the proposed method as well as the manual estimation in the field) of the validation trees (Figure 12). It was found that both models achieved comparable classification accuracy on the validation dataset, as assessed by the R^2 value (0.69 for Algorithm 1 and 0.72 for gradient boost model), indicating a good fit between the ground truth and calculated yellowness. However, Algorithm 1 exhibited significantly slower processing speed compared to the Gradient Boost method. On the same point cloud, Gradient Boost model was approximately six times faster (with average segmentation time of 0.39 sec per tree) compared to Algorithm 1 (2.41 sec per tree). Consequently, Gradient Boost was selected as the optimal model for subsequent point cloud segmentation of all trees from all weeks of data collection. Figure 13 demonstrates the results from the gradient boost segmentation model for a test tree during weeks 1, 3, and 5.

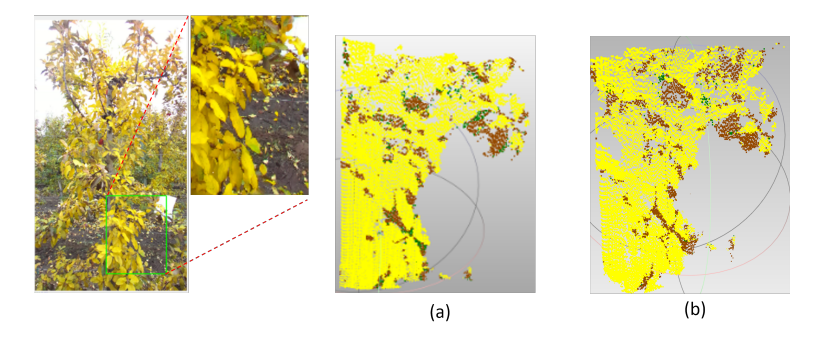


Figure 11: Example segmented point cloud of tree canopies in the validation data. The region delineated by the green rectangle was cropped and the corresponding color image and point cloud data was extracted for performance assessment. The results from the segmentation models on the cropped point cloud are shown in a) Algorithm 1; and b) Gradient Boost Classifier. The three colors in the point cloud represent three groups; green leaves, yellow leaves, and trunk.

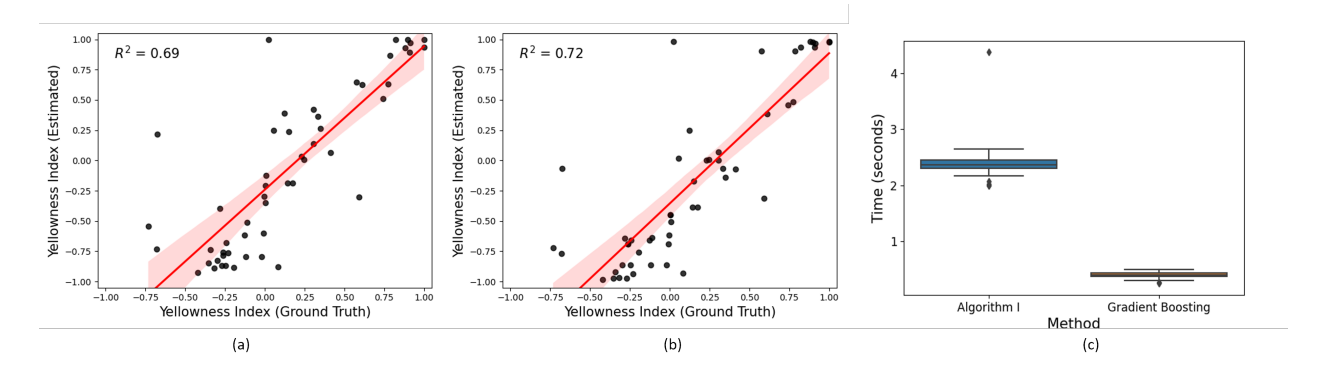


Figure 12: Performance of two classification/clustering models on the validation dataset; a) Estimated vs ground truth yellowness indexachieved by Algorithm 1; b) Same achieved by Gradient Boost; and c) Processing time (per image) on thirty-five test trees across all five weeks of data collection in 2023.

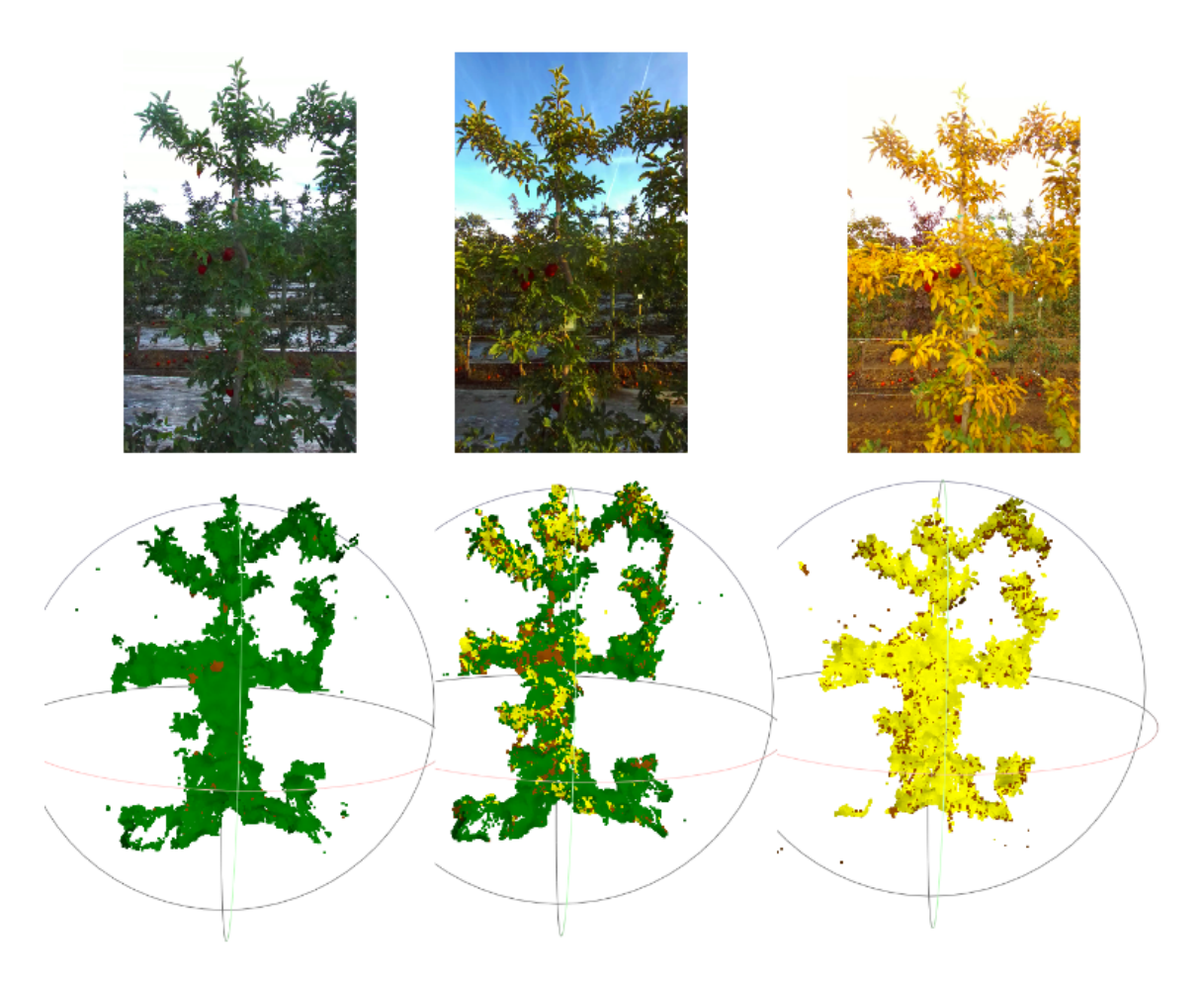


Figure 13: The images (top row) and segmented point cloud (bottom row) of a test tree during weeks 1,3, and 5. The three colors in the point cloud represent three groups; green-green leaves, yellow-yellow leaves, and brown-trunk, branches and some leaves that have turned brown.

3.2. Yellowness Index and Leaf Nitrogen Concentration

The segmented point clouds were used to calculate yellowness index for each tree over individual weeks of image collection using equation 1. Spatial maps of these yellowness indices were depicted in Figure 14, which shows the pattern and progression of yellowing of the trees during fall, 2021 (Figure 14 a) and fall, 2023 (Figure 14 b). The darker points in these maps represent greener trees and the lighter points represent yellower trees. A consistent trend of increasing yellowness index over time is noticed in both years. However, it was noticed that the yellowing trends were different between two years. In 2021, trees showed early transition to yellow in week 2 (around October 22), whereas in 2023, this change occurred later, nearly after three weeks (after November 10). This difference could potentially be attributed to relatively higher temperature during the growing season in 2021 compared to 2023 (Figure 15, AgWeatherNet) as shown by the cumulative growing degree days (GDDS). Growing degree days (GDDs) are calculated by averaging the day's maximum and minimum temperatures, subtracting a crop-specific base temperature below which growth ceases, and summing these values over the season (Miller et al., 2001). This method provides a more precise measure of plant growth stages than calendar days, as it accounts for the variable influence of temperature on developmental rates, allowing for more accurate predictions of phenological events regardless of annual temperature fluctuations. Prior studies by De la Haba et al. (2014) and Kim et al. (2020) have highlighted the impact of higher temperatures on senescence, indicating that elevated temperatures can induce early senescence in foliage. The timing of full bloom differed by almost three weeks between the years, with blooms on April 13 in 2021 and May 2 in 2023. This difference in bloom timing correlates with the observed variations in the timing of tree yellowing, further supporting the role of GDDs in influencing key phenological stages. In both years, yellowing occurred approximately 29 weeks after full bloom. Combining temperature data with bloom dates could provide a prediction tool to estimate monitoring window for fall color changes in apple trees, which is essential for the practical application of the yellowness index in optimizing N application.

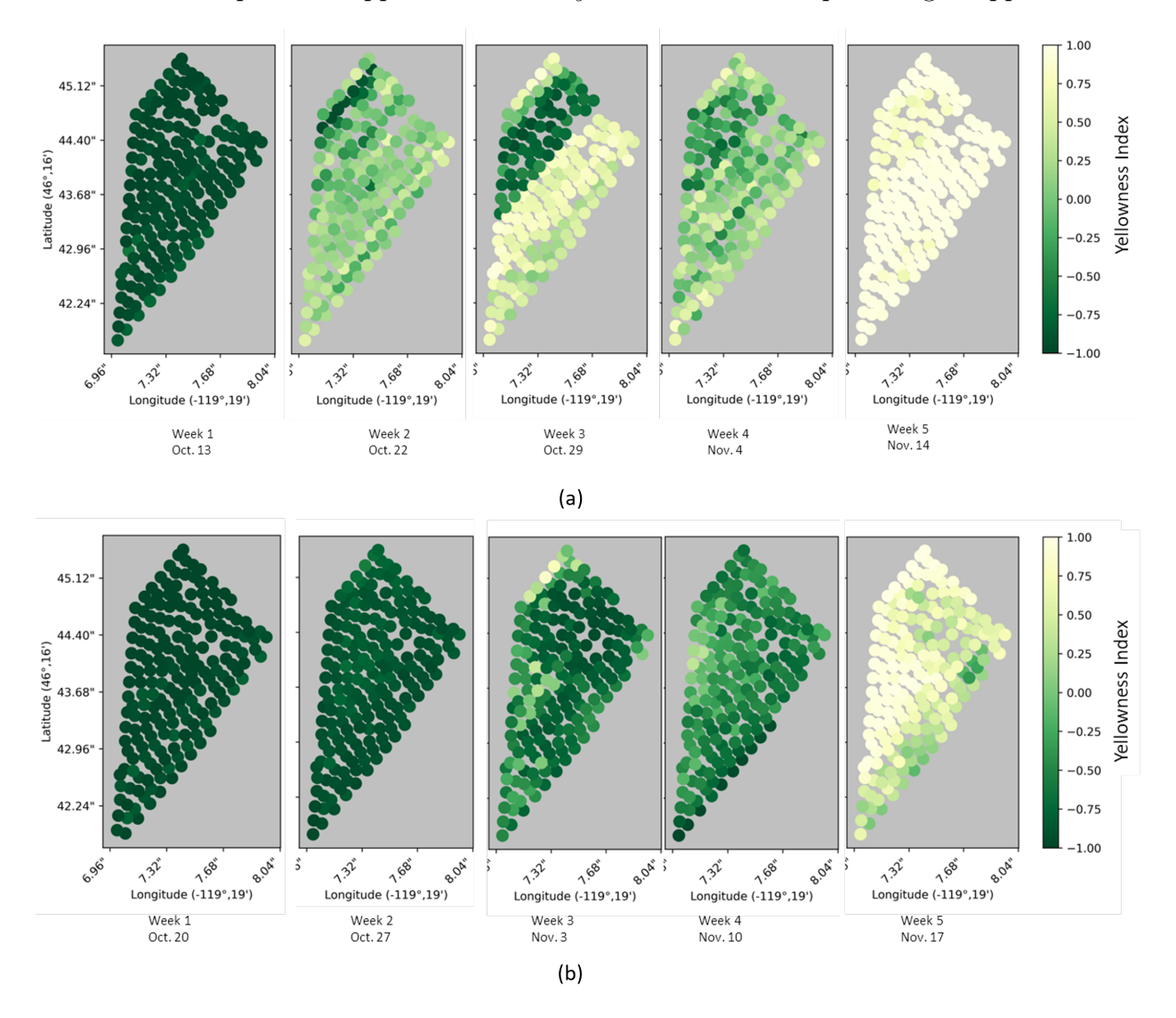


Figure 14: Spatial variation of *yellowness index* over the study period in the test orchard; a) 2021 and b) 2023 datasets. The color bar on the right indicates the yellowness level, with darker shade representing greener trees and lighter shade representing yellower trees.

To explore the potential of color transformation in estimating N status in apple trees, correlation between leaf nitrogen concentrations and yellowness was investigated. Figure 16 shows leaf nitrogen concentrations plotted against the *yellowness index* for all five weeks of data collection in a)2021; and b) 2023. The points in scatter plots were categorized into five groups based on leaf nitrogen concentrations, as outlined in Section 3.2. In general,

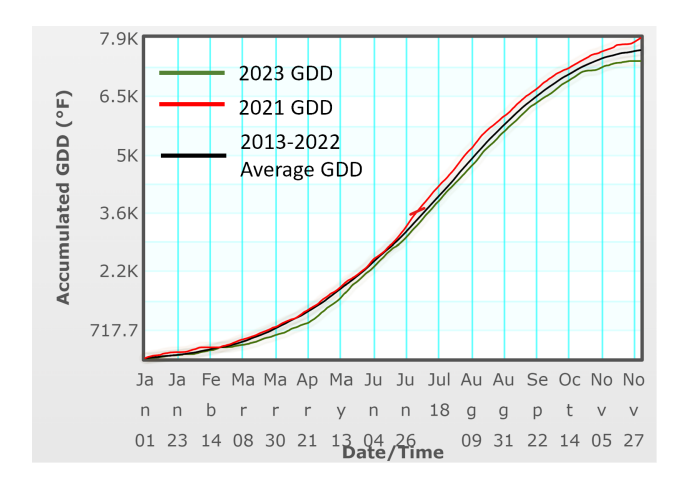


Figure 15: Growing degree days during 2021 and 2023 (AgWeatherNet). The red line shows the cumulative growing degree days for 2021 the green line shows that for 2023. The black line shows the average cumulative growing degree days between 2013 and 2022.

higher nitrogen levels in trees corresponded to lower *yellowness index* in both years (r values ranging from -0.28 to -0.43 in 2021 and 0.16 and -0.64 in 2023), and an extended retention of greenness in tree foliage with higher N content compared to those with lower N levels. This finding confirms with existing literature emphasizing that trees with higher nitrogen levels tend to maintain green foliage color longer (Shi et al., 2021; Wen et al., 2018; Li et al., 2022).

Qualitative resemblance of leaf nitrogen concentration and yellowness index can also be seen in Figure 17 (a – week 4 of 2021; b – week 5 of 2023). In both plots, red ellipses represent areas with higher leaf N and black ellipses represent areas with lower leaf N. It can be noticed in both of these plots that the area with lower leaf Nitrogen (right plots - black ellipses) has higher yellowness indices in the left plots and vice versa. These findings indicate that the yellowness index of trees estimated at different weeks during senescence can be a strong indicator of the nitrogen status in the tree, suggesting that leaf nitrogen content plays a crucial role in determining tree yellowness, which can be accurately captured by the yellowness index metric.

The results from the one-way ANOVA suggested that a significant difference between the group means existed in weeks 1, 3, and 4 of 2021 and weeks 2, 4, and 5 of 2023, all at a

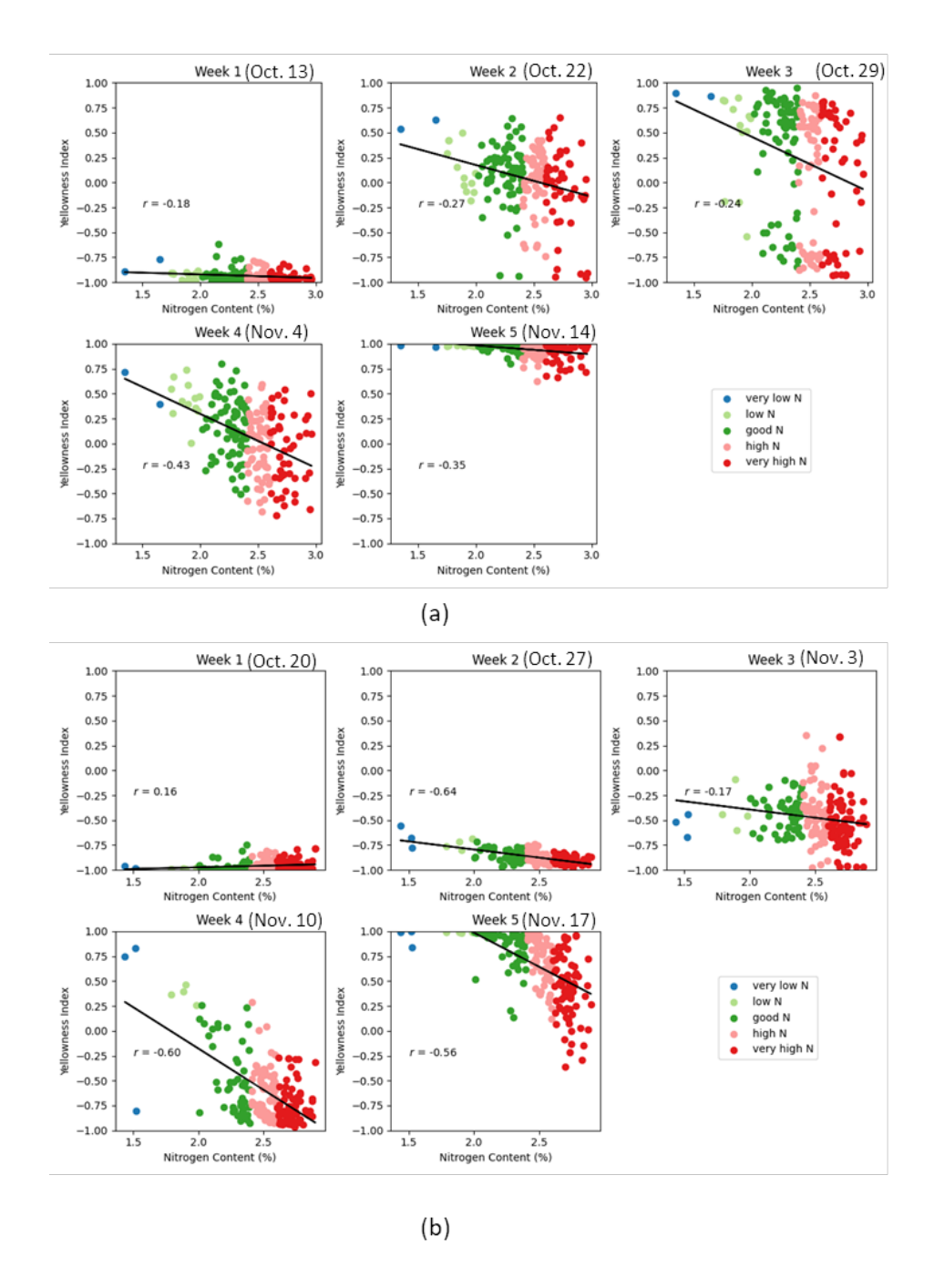


Figure 16: yellowness index over weeks during the fall season of (a) 2021 and (b) 2023 in trees shown with Nitrogen % in the trees. (Very low N (N < 1.7%), Low N (1.7% < N < 2.0%), Good N (2% < N < 2.4%), High N(2.4% < N < 2.6%), Very high N (N > 2.6%). The dates on the plots show the date when the data was collected in 2021 and 2023.

significance level of p < 0.05. Subsequently, post hoc analysis via TukeyHSD tests at the same significance level was conducted (Table 1). Rows shown in the table indicate that there

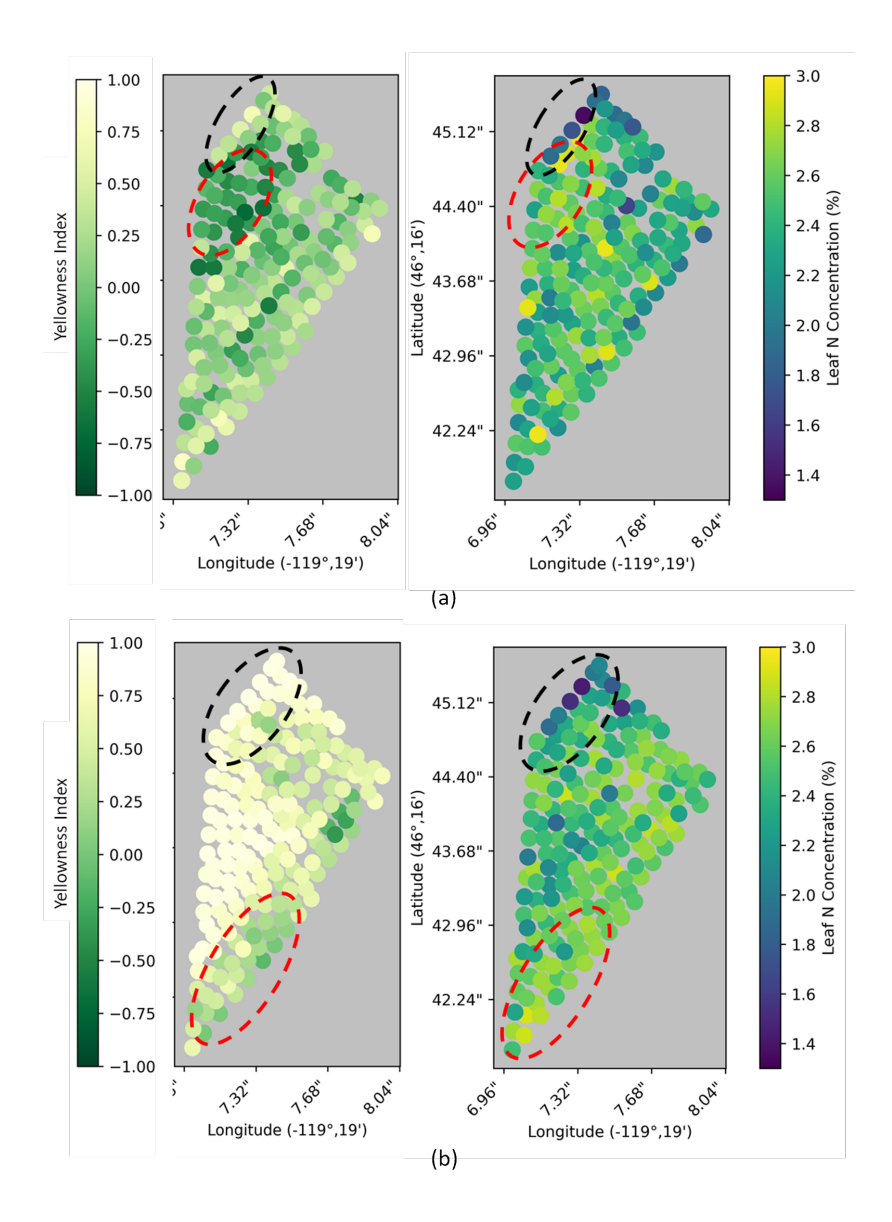


Figure 17: Yellowneness Index (left plots) variation with leaf nitrogen concentrations (right plots) in (a) week 4 of 2021, and (b)week 5 of 2023. The colorbars on the left and right show the values of yellowess index and leaf nitrogen concentrations. The red ellipses show the sample areas with higher nitrogen concentrations, and the black ellipses show areas with lower nitrogen concentrations.

existed a significant difference in group means between values in Column Group 1 and Group 2 at the given week. Significant differences in yellowness index between trees with different nitrogen levels were most prominent during weeks 2 and 4 in 2023 and week 4 in 2021.

These findings underscored the significance of timing the yellowness estimation in distinguishing trees with different nitrogen levels. To establish a more robust method for predicting

these significant periods of observation for each cropping season, it's essential to consider various factors such as growing degree days, precipitation, and average temperature. By identifying the critical time points (in terms of days after full bloom or growing degree days) when significant differences in leaf color occur between trees at different nitrogen concentrations, the yellowness index measured at those specific times would be crucial for accurately assessing tree nitrogen status.

Table 1: Post-hoc analysis (Tukey test) between trees at different N concentrations when divided into 3 and 5 classes based on leaf Nitrogen concentrations at a) 2021 and b) 2023. The given rows showed significant differences between Group 1 and Group 2 in the column during the given week at a significance level of p < 0.05.

Weeks	Year			
	2021		2023	
	Group 1	Group 2	Group 1	Group 2
Week1	Low	Very High		
Week 2	-	-	Very Low	Good
			Very Low	High
			Very Low	Very High
			Low	Good
			Low	High
			Low	Very High
			Good	High
			Good	Very High
Week 3	Low	Very High	-	-
	Good	Very High		
Week 4	Low	High	Very Low	Low
	Low	Very High	Very Low	High
	Good	High	Very Low	Very High
	Good	Very High	Low	Good
			Low	High
			Low	Very High
			Good	High
			Good	Very High
Week 5	-	-	Very Low	Low
			Very Low	Good
			Very Low	High
			Very Low	Very High

The results from this study demonstrated that a machine vision system could be used to identify the critical differences in the yellowing patterns of the trees and could be used as a predictor of nitrogen levels in apple trees. The outcomes and methodologies of this study offer a means to quantify tree color and determine tree nitrogen levels, which are crucial factors in guiding fertilizer application to individual trees. However, the system relies on a machine vision system which is susceptible to variations in external lighting conditions. Nevertheless, recent advancements in machine vision sensors have addressed low-light conditions using

innovative techniques such as high dynamic range (Zhang et al., 2020, 2021) and Adversarial Networks (Chen et al., 2018). In addition, deep learning methods have notably enhanced imaging system resilience to diverse lighting environments (Li et al., 2021a,b). The algorithm employed in this study relies on labeled data for initially training the model to differentiate yellow and green points on trees, necessitating manual inputs. It's important to note that this algorithm might require further calibration between different years and across tree varieties for optimal performance.

4. Conclusion and Future Work

Leaf Nitrogen concentration is one of the critical factors that determines the yield and quality of fruits and the overall health of the apple trees. Growers often rely on different visual cues including the canopy color for assessing plant health and nitrogen needs. This study presented a machine vision-based approach for quantitatively assessing tree canopy color and utilizing the color during transitional period in the fall (when the leaves change color from green to yellow during senescence) to assess N status in trees. Specifically, this study segmented the test tree canopies in an outdoor environment with natural background using 3D point clouds, identified yellow and green regions in the canopy using a gradient boost model, and used a metric called *yellowness index* to quantify the canopy color. It was found that leaf nitrogen concentration in apple trees was significantly correlated to the yellowness index of the tree canopies at the optimal color change stage in the fall. The trees notably began transitioning in color around the 29th week following full bloom in both years the test was conducted. The trees with lower and higher nitrogen showed the significant differences between the yellowness indices during week 4 (Around November 4) in 2021 and week 2 (October 27) and week 4 (November 10) in 2023. The difference in these dates signifies the importance of factors such as temperature, humidity, and growing degree days during different years in predicting optimal window of estimate yellowness index for tree nitrogen levels assessment. Overall, the findings from this study could be summarized as:

- 1. A machine vision-based system could be used to segment the yellow and green foliage in apple trees in outdoor orchard environments. A metric yellowness index was defined to quantify the status of tree foliage color, which was estimated with a R^2 value of 0.72 using a gradient boost classifier model.
- 2. The yellowness index of the trees was found to be correlated with the leaf nitrogen levels in the trees. Trees with different nitrogen levels showed different yellowing patterns. The difference between low and high nitrogen trees were more significant (p < 0.05) in week 4 in 2021(31 weeks after full bloom) and 2023 (29 weeks after full bloom).

This study presented a novel way of assessing the color of apple tree canopies and explored its relationship with leaf Nitrogen concentration. This method could be a good alternative to traditional methods like chemical methods, chlorophyll meter, and spectral analysis of N assessment in apple trees and can give instantaneous results that could be expanded to individual tree level assessment using a ground vehicle or robot. The study also provided critical insights into the fall color changes in apple trees and their relationship with leaf nitrogen concentrations.

One major limitation of assessing leaf nitrogen level using the proposed method is that some years, the tree might freeze early due to rapid decline in temperature and never show the color change. In such cases, it is important to not rely on just a single factor and have a decision support system that takes multiple features as input, making the decision more robust and reliable. The *yellowness index* values along with other commonly used visual features like canopy density, trunk cross-sectional area, and shoot length can be combined into a single robust model and could aid in developing a robust decision support system for efficient fertilization plans tailored to individual tree nitrogen needs.

For practical implementation, machinery capable of delivering nutrients at a per-tree level becomes essential. Several companies and academic institutions are developing autonomous systems for precise orchard operations (Brown et al., 2024). Integrating the findings from

this study into such machinery would provide a comprehensive solution for growers to apply right amount of N to individual trees thus substantially enhancing tree health, and fruit yield and quality, and ultimately increase returns while insuring long term sustainability of apple production.

Acknowledgement

This research was supported by the Washington Tree Fruit Research Commission. Special thanks to David Allan for providing access to the test orchard and for valuable feedback and support during this work.

References

Aggelopoulou, K., Wulfsohn, D., Fountas, S., Gemtos, T., Nanos, G., Blackmore, S., 2010. Spatial variation in yield and quality in a small apple orchard. Precision agriculture 11, 538–556.

AgWeatherNet, . Wheat grain gdds. URL: https://smallgrains.wsu.edu/weather-resources/wheat-grain-growing-degree-day-calculator/.

Ali, M., Al-Ani, A., Eamus, D., Tan, D., 2012. Leaf nitrogen determination using handheld meters, in: Australian Agronomy Conference.

Arnó, J., Martínez-Casasnovas, J.A., Uribeetxebarria, A., Escolà, A., Rosell-Polo, J.R., 2017. Comparing efficiency of different sampling schemes to estimate yield and quality parameters in fruit orchards. Advances in Animal Biosciences 8, 471–476. doi:10.1017/S2040470017000978. publisher: Cambridge University Press.

Baret, F., Fourty, T., 1997. Radiometric estimates of nitrogen status of leaves and canopies, in: Diagnosis of the nitrogen status in crops. Springer, pp. 201–227.

Bartlett, P., Freund, Y., Lee, W.S., Schapire, R.E., 1998. Boosting the margin: A new explanation for the effectiveness of voting methods. The annals of statistics 26, 1651–1686.

- Brown, J., Paudel, Α., Biehler, D., Thompson, Α., Karkee. М., Grimm, C., Davidson, J.R., 2024. Tree detection and in-row localization for autonomous precision orchard management. Computers and Electronics in Agriculture 227, 109454. URL: https://www.sciencedirect.com/science/article/pii/ S0168169924008457, doi:https://doi.org/10.1016/j.compag.2024.109454.
- Chen, Y.S., Wang, Y.C., Kao, M.H., Chuang, Y.Y., 2018. Deep photo enhancer: Unpaired learning for image enhancement from photographs with gans, in: Proceedings of the IEEE conference on computer vision and pattern recognition, pp. 6306–6314.
- Cheng, L., 2010. When and how much nitrogen should be applied in apple orchards. New York Fruit Quarterly 18, 25–28.
- Cheng, L., Schupp, J., 2004. Nitrogen fertilization of apple orchards.
- Cho, S.E., 2010. Probabilistic assessment of slope stability that considers the spatial variability of soil properties. Journal of geotechnical and geoenvironmental engineering 136, 975–984.
- Ferguson, I.B., Triggs, C.M., 1990. Sampling factors affecting the use of mineral analysis of apple fruit for the prediction of bitter pit. New Zealand Journal of Crop and Horticultural Science 18, 147–152. doi:10.1080/01140671.1990.10428086.
- De la Haba, P., De la Mata, L., Molina, E., Agüera, E., 2014. High temperature promotes early senescence in primary leaves of sunflower (helianthus annuus l.) plants. Canadian Journal of Plant Science 94, 659–669.
- James A. Taylor, John-Paul Praat, A. Frank Bollen, 2007. Spatial Variability of Kiwifruit Quality in Orchards and Its Implications for Sampling and Mapping in: HortScience Volume 42 Issue 2 (2007) URL: https://doi.org/10.21273/HORTSCI.42.2.246.

- Kim, C., Kim, S.J., Jeong, J., Park, E., Oh, E., Park, Y.I., Lim, P.O., Choi, G., 2020. High ambient temperature accelerates leaf senescence via phytochrome-interacting factor 4 and 5 in arabidopsis. Molecules and cells 43, 645.
- Kirk, P.L., 1950. Kjeldahl method for total nitrogen. Analytical chemistry 22, 354–358.
- Klein, I., Levin, I., Bar-Yosef, B., Assaf, R., Berkovitz, A., 1989. Drip nitrogen fertigation of 'starking delicious' apple trees. Plant and soil 119, 305–314.
- Lee, D.W., 2002. Anthocyanins in autumn leaf senescence.
- Li, C., Guo, C., Han, L., Jiang, J., Cheng, M.M., Gu, J., Loy, C.C., 2021a. Low-light image and video enhancement using deep learning: A survey. IEEE transactions on pattern analysis and machine intelligence 44, 9396–9416.
- Li, C., Guo, C., Loy, C.C., 2021b. Learning to enhance low-light image via zero-reference deep curve estimation. IEEE Transactions on Pattern Analysis and Machine Intelligence 44, 4225–4238.
- Li, W., Zhu, X., Yu, X., Li, M., Tang, X., Zhang, J., Xue, Y., Zhang, C., Jiang, Y., 2022. Inversion of nitrogen concentration in apple canopy based on uav hyperspectral images. Sensors 22, 3503.
- Mahmud, M.S., Zahid, A., He, L., Choi, D., Krawczyk, G., Zhu, H., Heinemann, P., 2021. Development of a lidar-guided section-based tree canopy density measurement system for precision spray applications. Computers and Electronics in Agriculture 182, 106053. doi:https://doi.org/10.1016/j.compag.2021.106053.
- Miller, P., Lanier, W., Brandt, S., 2001. Using growing degree days to predict plant stages. Ag/Extension Communications Coordinator, Communications Services, Montana State University-Bozeman, Bozeman, MO 59717, 994–2721.

- Murneek, A.E., Logan, J., 1932. Autumnal migration of nitrogen and carbohydrates in the apple tree with special reference to leaves. University of Missouri, College of Agriculture, Agricultural Experiment Station.
- Naschitz, S., Naor, A., Wolf, S., Goldschmidt, E.E., 2014. The effects of temperature and drought on autumnal senescence and leaf shed in apple under warm, east mediterranean climate. Trees 28, 879–890.
- Natekin, A., Knoll, A., 2013. Gradient boosting machines, a tutorial. Frontiers in neuro-robotics 7, 21.
- Neilsen, G.H., Neilsen, D., Herbert, L., 2009. Nitrogen fertigation concentration and timing of application affect nitrogen nutrition, yield, firmness, and color of apples grown at high density. HortScience 44, 1425–1431.
- Paudel, A., Davidson, J.R., Grimm, C., Karkee, M., 2023. Vision-based normalized canopy area estimation for variable nitrogen application in apple orchards. Smart Agricultural Technology 5, 100309.
- Paudel, A., Karkee, M., Davidson, J.R., Grimm, C., 2022. Canopy density estimation of apple trees. IFAC-PapersOnLine 55, 124–128.
- Raese, J.T., Drake, S.R., Curry, E.A., 2007. Nitrogen fertilizer influences fruit quality, soil nutrients and cover crops, leaf color and nitrogen content, biennial bearing and cold hardiness of 'golden delicious'. Journal of plant nutrition 30, 1585–1604.
- Sallato, B., 2017. Leaf tissue analysis. URL: https://treefruit.wsu.edu/orchard-management/soils-nutrition/leaf-tissue-analysis/.
- Sanchez, E.E., Khemira, H., Sugar, D., Righetti, T., 1995. Nitrogen management in orchards.
- Shi, P., Wang, Y., Xu, J., Zhao, Y., Yang, B., Yuan, Z., Sun, Q., 2021. Rice nitrogen nutrition

- estimation with rgb images and machine learning methods. Computers and Electronics in Agriculture 180, 105860.
- Spencer, P.W., 1973. Apple leaf senescence: leaf disc compared to attached leaf. Plant physiology 51, 89–92.
- Thompson, D., 2017. How to Use Color Spaces to Talk About Color First Source Worldwide.

 URL: https://www.fsw.cc/color-spaces/.
- Treder, W., Klamkowski, K., Kowalczyk, W., Sas, D., Wojcik, K., et al., 2016. Possibilities of using image analysis to estimate the nitrogen nutrition status of apple trees. Zemdirbyste-Agriculture 103, 319–326.
- Umali, B.P., Oliver, D.P., Forrester, S., Chittleborough, D.J., Hutson, J.L., Kookana, R.S., Ostendorf, B., 2012. The effect of terrain and management on the spatial variability of soil properties in an apple orchard. Catena 93, 38–48.
- UniversityofArizona, . Nitrogen management guide for apples. URL: chrome-extension: //efaidnbmnnnibpcajpcglclefindmkaj/https://ag.arizona.edu/crop/soils/aznapples.pdf.
- Wachs, J.P., Stern, H.I., Burks, T., Alchanatis, V., 2010. Low and high-level visual feature-based apple detection from multi-modal images. Precision Agriculture 11, 717–735.
- Van der Walt, S., Schönberger, J.L., Nunez-Iglesias, J., Boulogne, F., Warner, J.D., Yager, N., Gouillart, E., Yu, T., 2014. scikit-image: image processing in python. PeerJ 2, e453.
- Wang, T., Sankari, P., Brown, J., Paudel, A., He, L., Karkee, M., Thompson, A., Grimm, C., Davidson, J., Todorovic, S., 2023. Automatic estimation of trunk cross sectional area using deep learning. Collaborative Robotics & Intelligent Systems Institute, Oregon State University.

- Wang, Z., Underwood, J., Walsh, K.B., 2018. Machine vision assessment of mango orchard flowering. Computers and Electronics in Agriculture 151, 501–511.
- Wen, X., Zhu, X., Cao, S., Guo, X., Yu, R., Xiong, J., Gao, D., 2018. Nitrogen estimation model of apple leaves based on imaging spectroscopy. Remote Sensing Science 6.
- Wulfsohn, D., Aravena Zamora, F., Potin Téllez, C., Zamora Lagos, I., García-Fiñana, M., 2012. Multilevel systematic sampling to estimate total fruit number for yield forecasts. Precision Agriculture 13, 256–275. URL: https://doi.org/10.1007/s11119-011-9245-2, doi:10.1007/s11119-011-9245-2.
- Ye, X., Abe, S., Zhang, S., 2020. Estimation and mapping of nitrogen content in apple trees at leaf and canopy levels using hyperspectral imaging. Precision Agriculture 21, 198–225.
- Zhang, S., Zhang, Y., Jiang, Z., Zou, D., Ren, J., Zhou, B., 2020. Learning to see in the dark with events, in: Computer Vision–ECCV 2020: 16th European Conference, Glasgow, UK, August 23–28, 2020, Proceedings, Part XVIII 16, Springer. pp. 666–682.
- Zhang, Y., Guo, X., Ma, J., Liu, W., Zhang, J., 2021. Beyond brightening low-light images. International Journal of Computer Vision 129, 1013–1037.
- Zhou, Q.Y., Park, J., Koltun, V., 2018. Open3d: A modern library for 3d data processing. arXiv preprint arXiv:1801.09847.